Molecular Cancer Therapeutics

Vitamin D Enhances the Efficacy of Irinotecan through miR-627–Mediated Inhibition of Intratumoral Drug Metabolism

Meiyan Sun, Qunshu Zhang, Xiaoyu Yang, Steven Y. Qian, and Bin Guo

Abstract

Cytochrome P450 enzyme CYP3A4 is an important drug-metabolizing enzyme, and high levels of tumoral expression of CYP3A4 are linked to drug resistance. We investigated the function of vitamin D–regulated miR-627 in intratumoral CYP3A4 suppression and its role in enhancing the efficacy of chemotherapy. We found that miR-627 targets CYP3A4 and suppresses CYP3A4 expression in colon cancer cell lines. Furthermore, calcitriol (the active form of vitamin D) suppressed CYP3A4 expression by activating miR-627. As a result, calcitriol inhibited CYP3A4-mediated metabolism of irinotecan (a topoisomerase I inhibitor) in cancer cells. We show that calcitriol enhanced the efficacy of irinotecan in growth inhibition and apoptosis induction. When miR-627 is inhibited, calcitriol fails to enhance the activity of irinotecan. In addition, overexpression of miR-627 or siRNA knockdown of CYP3A4 enhanced the efficacy of irinotecan in growth inhibition and apoptosis induction. In contrast, overexpression of CYP3A4 abolished the effects of calcitriol on the activity of irinotecan. Using a nude mouse xenograft model, we demonstrated that calcitriol inhibited CYP3A4 and enhanced the *in vivo* antitumor activity of irinotecan without causing side effects. Our study identified a novel target for improving cancer therapy, i.e., modulating the intratumoral CYP3A4-mediated drug metabolism with vitamin D. This strategy could enhance the therapeutic efficacy without eliciting the side effects. *Mol Cancer Ther; 15(9); 2086–95. ©2016 AACR.*

Introduction

Drug resistance is a major problem that prevents chemotherapy from achieving satisfying responses in patients. Traditionally, studies on drug resistance have focused on mechanisms including multidrug resistance mediated by multidrug resistance–associated protein 1 (MRP1; ref. 1) and P-glycoprotein (2), resistance to apoptosis mediated by antiapoptotic proteins (3), amplification of drug target genes (4), etc. However, a potentially significant drug resistance mechanism, cytochrome P450–mediated intratumoral drug metabolism, has received minimal attention.

Cytochrome P450 3A4 (CYP3A4) is one of the most abundant P450 enzymes expressed in human liver and the gastrointestinal tract. CYP3A4 contributes to the metabolism of approximately 50% the drugs currently used in the clinic (5). In cancer chemotherapy, CYP3A4 has been associated with drug inactivation, and high levels of tumoral expression of CYP3A4 are linked to drug resistance and poor response to therapy (6–10). Irinotecan, a camptothecin derivative, is one of the major drugs used for the treatment of colorectal cancers (11). Irinotecan is metabolized in cancer cells by carboxylesterase (CE) into the active metabolite SN-38, and by CYP3A4 into the inactive metabolites 7-ethyl-10-[4-(1-piperidino)-1-amino]-carbonyloxy camptothecin (NPC) and 7-ethyl-10-[4-N-(5-aminopentanoic acid)-1-piperidino]-carbonyloxycamptothecin (APC; ref. 12), with APC as the major inactive metabolite. SN-38 induces CYP3A4 overexpression in colon cancer by activating the steroid and xenobiotic receptor (SXR), subsequently leading to resistance to irinotecan (13). Furthermore, CYP3A4 expression is increased in colon cancer cells that exhibit cancer stem cell–like characters (14), potentially contributing to multidrug resistance. Importantly, CYP3A4 is expressed at substantially higher levels in the normal colon and colon cancers than those in the liver (15), indicating that the intratumoral CYP3A4 may play a critical role in drug metabolism and resistance to chemotherapy in colon cancer.

Preclinical research has demonstrated clear antitumor activities of vitamin D against various types of cancers, including colon cancer (16). Vitamin D analogues have been shown to enhance the antitumor activity of irinotecan in a colon cancer nude mouse xenograft model (17), even though the underlying mechanism is not clear. We recently identified miR-627 as the sole miRNA whose expression was significantly increased by calcitriol ($1\alpha,25(OH)_2D_3$, the active form of vitamin D) in colon cancer cells (18). MiRNAs are small single-stranded noncoding RNAs that silence target genes by cleaving mRNA molecules or inhibiting translation (19). Studies have shown that miRNAs can regulate cancer pathogenesis, cell-cycle progression (20, 21), differentiation (22, 23), metabolism (24, 25), invasion and metastasis (26, 27), as well as apoptosis (28, 29). We further demonstrated that miR-627 targets CYP3A4 and suppresses CYP3A4 expression. Because CYP3A4 is

Department of Pharmaceutical Sciences, North Dakota State University, Fargo, North Dakota.

Note: Supplementary data for this article are available at Molecular Cancer Therapeutics Online (http://mct.aacrjournals.org/).

Corresponding Author: Bin Guo, North Dakota State University, NDSU School of Pharmacy, NDSU Dept 2665, PO Box 6050, Fargo, ND 58108. Phone: 701-231-5164; Fax: 701-231-8333; E-mail: Bin.Guo@ndsu.edu

doi: 10.1158/1535-7163.MCT-16-0095

AACR

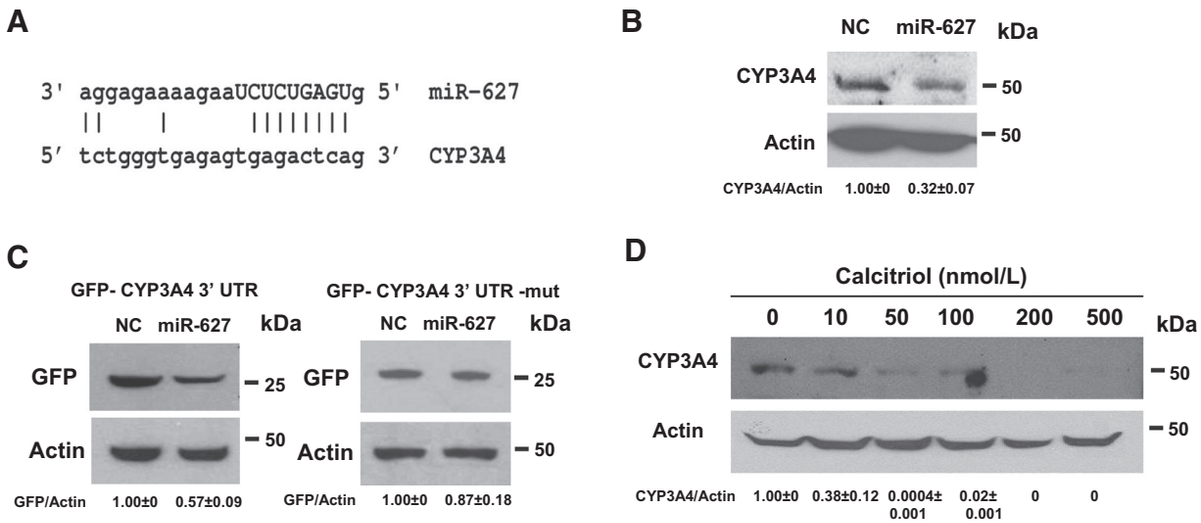

Figure 1.

miR-627 targets CYP3A4. **A,** predicted duplex formation between human *CYP3A4* 3′UTR and miR-627. **B,** HCT-116 cells were transfected with negative control or miR-627 mimics. Forty-eight hours after transfection, cell lysates were analyzed by Western blots with the indicated antibodies. The experiment was repeated 3 times. **C,** HCT-116 cells were transfected with GFP-*CYP3A4* 3′UTR (left) or GFP-*CYP3A4* 3′UTR-mut (right) plasmids together with negative control miRNA or miR-627 mimics. Western blotting was performed with anti-GFP and anti-actin antibodies. Relative protein levels were quantified and shown under the gel. The experiment was repeated 3 times. **D,** HT-29 cells were treated with various doses of calcitriol for 48 hours, and Western blots were done using the indicated antibodies. Relative protein levels were quantified and shown under the gel. The experiment was repeated 3 times. The mean and SD values of densitometric quantifications are shown.

responsible for the inactivation of irinotecan, we here report that by activating miR-627 to suppress CYP3A4, vitamin D can enhance the therapeutic efficacy of irinotecan to achieve better cancer suppression.

Materials and Methods

Cells and transfection

The cell lines HT-29 and HCT-116 were purchased from the American Type Culture Collection (ATCC) in 2004. HT-29 (ATCC HTB-38) was derived from a female Caucasian patient with colorectal adenocarcinoma. HCT-116 (ATCC CCL-247) was derived from a male patient with colorectal carcinoma. The cell lines were authenticated using short tandem repeat (STR) profiling in 2016 at Genetica. HCT-116 cells were cultured in RPMI1640 media containing 10% FBS. HT-29 cells were cultured in DMEM containing 10% FBS. For transient transfection, plasmids were transfected into cells using LipofectaminePlus Reagent (Invitrogen) following the manufacturer's protocol. MiRNA mimics were transfected into cells using X-treme GENE siRNA transfection reagent (Roche) following the manufacturer's protocol.

Drugs and chemicals

Irinotecan was purchased from Sigma. Calcitriol was purchased from Cayman Chemical.

Plasmid construction, siRNA, miRNA mimics, and inhibitors

The *CYP3A4* 3′UTR cDNA fragment was obtained by PCR using an expressed sequence tag clone as template. The PCR primers for the *CYP3A4* 3′UTR amplified a 430 bp sequence containing the miR-627 target site (forward: TGTCAGAACTAGAATTTGATTATTAACATA; reverse: CAGTTCTTTGTTACAAAATGTACGTG). The 3′UTR cDNA was inserted into pEGFP-C1 plasmid at the 3′ end of the EGFP cDNA (Xho I and BamH I). The pEGFP-C1-3′UTR plasmid containing a mutation within the miR-627 recognition site (ACTC to TGAG mutation within 3′UTR) was created by PCR using the QuickChange II site–directed mutagenesis Kit (Stratagene), following the supplied protocol. For the miR-627 sponge experiments, the 3′UTR cDNA was also inserted into pRNAT-CMV3.2/Puro plasmid (BamH I and Xho I) to create pRNAT-CMV3.2/Puro-3′UTR for stable transfection into HCT-116 cells. The pRNAT-CMV3.2/Puro-3′UTR-mut containing mutation within the miR-627 recognition site (ATTC to TGAG) in the 3′UTR was created by PCR using the QuickChange II site–directed mutagenesis Kit (Stratagene). To construct miRNA expression vectors, double-strand oligoes containing pre–miR-627 were cloned into pcDNA6.2-GW/EmGFP-miR plasmid (Invitrogen) by directional cloning. Negative control and CYP3A4 siRNAs were purchased from Ambion. Synthetic miRNA mimics (Pre-miR miRNA Precursors) for miR-627 (# AM17100) and negative control miR-NC (# AM17110) were purchased from Ambion.

LC/MS detection for irinotecan and its metabolites

LC/MS was performed as described previously (30). Chromatography grade acetonitrile (ACN), methanol, and water were purchased from EMD chemicals. Acetic acid (HOAc) was purchased from Sigma. Note that 100 μL culture medium from the cells treated by irinotecan for 48 hours was collected and then mixed with 100 μL ACN and methanol (v/v 1:1) spiked with internal standard, e.g., camptothecin (31). The mixture was vortexed and set on ice for 5 minutes, and then centrifuged at

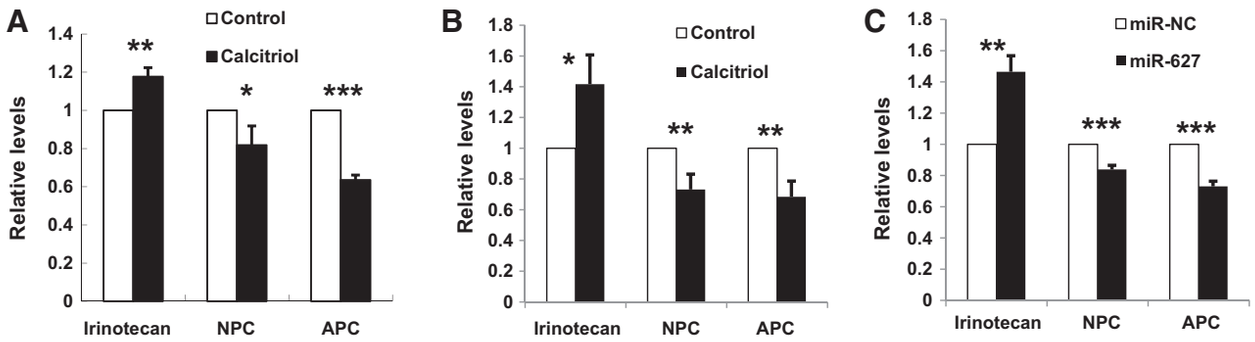

Figure 2.

Calcitriol inhibits CYP3A4-mediated metabolism of irinotecan. **A,** HT-29 cells were treated with or without 200 nmol/L of calcitriol for 24 hours, followed by 10 μmol/L irinotecan for additional 24 hours, and cell culture media were collected and analyzed by LC/MS as described in Materials and Methods. **B,** HCT-116 cells were treated with or without 200 nmol/L of calcitriol for 24 hours, followed by 10 μmol/L irinotecan for additional 24 hours, and cell culture media were collected and analyzed by LC/MS. **C,** HCT-116 cells stably expressing negative control miRNA or miR-627 were treated with 10 μmol/L irinotecan for 24 hours, and cell culture media were collected and analyzed by LC/MS. The experiment was repeated 3 times; representative results of three independent experiments are shown. Data shown are mean values + SD (*, $P < 0.05$; **, $P < 0.01$; and ***, $P < 0.001$).

13,000 rpm for 10 minute. After centrifugation, supernatant was filtered by syringe filter and transferred to micro-inserts for LC/MS analysis. The LC/MS system consisted of an Agilent 1200 series HPLC system and an Agilent 6300 LC/MSD SL ion trap mass system. Chromatography separations were performed on a ZORBAX Eclipse XDB-C18 column (Agilent; 3.5 μm, 75 × 4.6 mm) at 25°C with an injection volume of 20 μL with flow rate at 0.8 mL/min and mobile phase (A: water with 0.01% HOAc, and B: ACN with 0.01 % HOAc). Chromatography gradients were: (1) 0–12 minutes: 5%–40% B; (2) 12–15 minutes: 40%–90% B; (3) 15–17 minutes: 90%–5% B; (4) 17–20 minutes: 5% B. MS settings were as follows: electrospray ionization in positive mode; total ion current (TIC) chromatograms were performed in full mass scan mode (from m/z 300 to m/z 700); nebulizer pressure: 15.0 psi; dry gas flow rate: 5.0 L/min; dry temperature: 325∘C; compound stability: 20%; number of scans: 50.

Western blot analysis

Cells were lysed in RIPA buffer (1% NP-40, 0.5% sodium deoxycholate, 0.1% SDS in PBS). Complete protease inhibitor cocktail (Roche) was added to lysis buffer before use. Protein concentration was determined by Bio-Rad DC protein assay (Bio-Rad). Protein samples were subjected to SDS-PAGE and transferred to nitrocellulose membrane. The membrane was blocked in 5% nonfat milk in PBS overnight and incubated with primary antibody and subsequently with appropriate horseradish peroxidase–conjugated secondary antibody. Signals were developed with ECL reagents (Pierce) and exposure to X-ray films. Anti-CYP3A4 polyclonal antibody was purchased from Cell Signaling Technology. Anti–β-actin antibody was purchased from Sigma, and anti-GFP antibody was purchased from Santa Cruz Biotechnology. Image digitization and quantification were done with UN-SCAN-IT software from Silk Scientific.

WST-1 assay

Cell proliferation was measured by WST-1 assay (Roche) following the manufacturer's protocol. Briefly, at time of assay, WST-1 was added to the cell culture (10 μL per well in 96-well plate) and incubated for 4 hours. The plate was mixed for 1 minute on a shaker, and the absorbance of the formazan product was measured at 440 nm on a plate reader.

Detection of apoptosis

The Cell Death Detection Elisa^{PLUS} Kit (Roche) was used to detect apoptosis following the manufacturer's protocol. This assay determines apoptosis by measuring mono- and oligonucleosomes in the lysates of apoptotic cells. The cell lysates were placed into a streptavidin-coated microplate and incubated with a mixture of anti–histone-biotin and anti–DNA-peroxidase. The amount of peroxidase retained in the immunocomplex was photometrically determined with 2,2'-azino-bis(3-ethylbenzothiazoline-6-sulphonic acid) as the substrate. Absorbance was measured at 405 nm.

Isolation of CD133$^-$ HCT-116 cells

The CD133$^-$ HCT-116 cells were isolated by removing CD133-positive cells with anti-CD133 antibody (Miltenyi Biotec) using the EasySep Selection Kit from StemCell Technologies. This method uses magnetic nanoparticles to select cells expressing cell surface antigens that can be recognized by monoclonal antibodies. The purity of cell isolation was assessed with a BD FACSJazz flow cytometer.

Calculation of combination index

The combination index (CI) value was calculated using the CalcuSyn software (Biosoft). A CI < 1 represents synergism between two agents. CI = 1 and CI > 1 represent additivity and antagonism, respectively.

Vitamin D receptor signaling

Vitamin D receptor (VDR) signaling was measured using the Cignal Vitamin D Reporter (luc) Kit from Qiagen, following the manufacturer's protocol. The VDRE reporter (VDR-responsive luciferase) construct encodes the firefly luciferase reporter gene under the control of a minimal (m)CMV promoter and tandem repeats of the VDRE transcriptional response element, which monitors both increases and decreases in the transcriptional activity of VDR and hence the activity of the vitamin D signaling pathway.

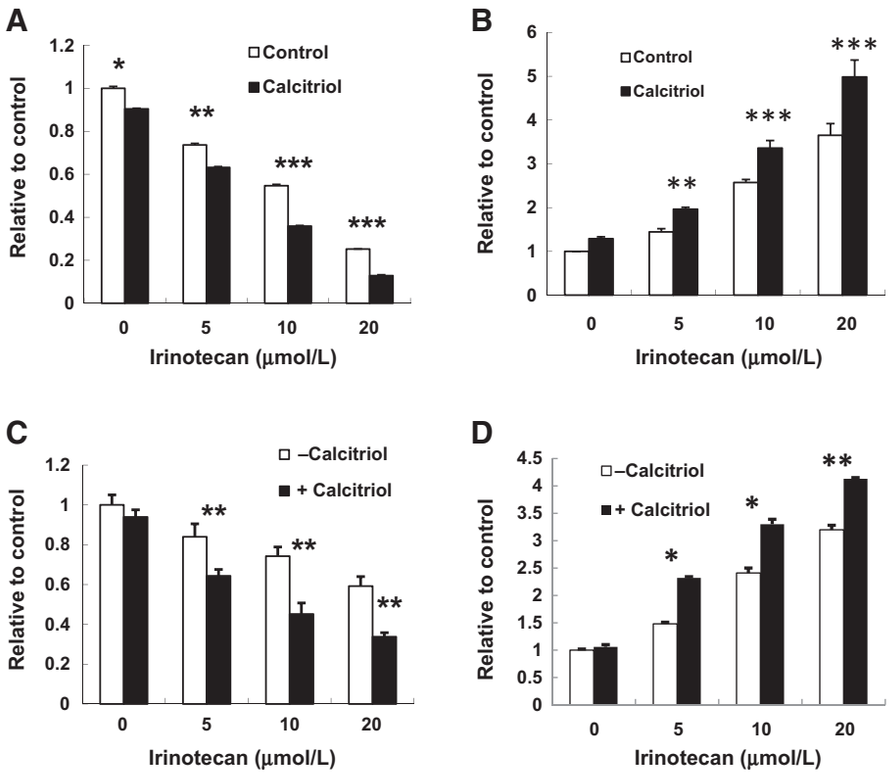

Figure 3.

Calcitriol enhances the antitumor activity of irinotecan in colon cancer cells. **A** and **B,** HT-29 cells were treated with or without 200 nmol/L calcitriol for 24 hours, followed by treatment with various doses of irinotecan for additional 24 hours. **A,** cell proliferation was assessed by WST-1 assay as described in Materials and Methods. Value of the control (0.213) was set as 1. **B,** apoptosis was assessed by Cell Death Detection Elisa assay as described in Materials and Methods. Value of the control (0.236) was set as 1. **C** and **D,** HCT-116 cells were treated with or without 200 nmol/L calcitriol for 24 hours, followed by treatment with various doses of irinotecan for additional 24 hours. **C,** cell proliferation was assessed by WST-1 assay. Value of the control (0.202) was set as 1. **D,** apoptosis was assessed by Cell Death Detection Elisa assay. Value of the control (0.377) was set as 1. All of the above experiments were repeated 3 times; data shown are mean values + SD (*, $P < 0.05$ and **, $P < 0.01$; ***, $P < 0.001$).

Measurement of blood calcium

Blood calcium level was measured with the Calcium Colorimetric Assay Kit from Biovision, following the manufacturer's protocol. This assay utilizes the chromogenic complex ($\lambda = 575$ nm) formed between calcium ions and 0-cresolphthalein to detect calcium levels in the range of 0.4–100 mg/dL.

Tumor xenografts in nude mice

Six- to 8-week-old male nude mice (Nu/Nu) were purchased from Charles River. The mice were maintained in sterile conditions using the Innovive IVC System from Innovive, following the protocol approved by the Institutional Animal Care and Use Committee of North Dakota State University. Tumor xenografts were established by subcutaneous injection of 2×10^6 cancer cells in the flank area of the mice. Calcitriol, irinotecan, and DMSO (as control) were administered by i.p. injection. Two axes of the tumor (L, longest axis; W, shortest axis) were measured with a caliper. Tumor volume was calculated as: $V = L \times W^2/2$.

Statistical analysis

Differences between the mean values were analyzed for significance using the unpaired two-tailed Student t test for independent samples. Correlation significance was assessed using Pearson's correlation coefficient test. $P \leq 0.05$ was considered to be statistically significant.

Results

Calcitriol-regulated miR-627 targets CYP3A4

We have recently identified miR-627 as the only miRNA whose expression level was significantly increased by calcitriol in colon cancer cells (18). Using the computational methods available at www.microrna.org and miRBase (http://microrna.sanger.ac.uk/), we identified *CYP3A4* gene as a potential target for miR-627. A recently published computational analysis also agreed with our assessment that miR-627 may target CYP3A4 (32). CYP3A4 is one of the most important drug-metabolizing enzymes (5), responsible for the first-pass metabolism, elimination time, and levels of drug exposure of many drugs including anticancer agents. The *CYP3A4* mRNA contains a 3′UTR sequence that is partially complementary to miR-627 (Fig. 1A). CYP3A4 expressed in tumor cells metabolizes irinotecan and contributes to tumor resistance to irinotecan (13). The potential effects of CYP3A4 on the antitumor activity of irinotecan make it an interesting target of miR-627. To confirm that miR-627 targets CYP3A4, we transfected HCT-116 cells with negative control or synthetic miR-627 mimics. Overexpression of miR-627 decreased CYP3A4 protein in the cells (Fig. 1B). When a cDNA fragment containing the 3′UTR sequence of *CYP3A4* was inserted downstream of the *GFP* gene in the pEGFP-C1 plasmid and the plasmid was transfected into HCT-116 cells together with pcDNA6.2-GW-miR-627 (to overexpress miR-627), GFP expression was reduced by miR-627, but not by the negative control miRNA expressed in pcDNA6.2-GW–negative-control plasmids (Fig. 1C, left). The action of the miR-627 was dependent on the miRNA binding site within the *CYP3A4* 3′UTR, since GFP expression was reduced to a much lesser degree by the miRNA when the binding site was mutated (Fig. 1C, right). If miR-627 targets *CYP3A4*, then calcitriol should decrease CYP3A4 since it induces miR-627 expression. Indeed, treatment with calcitriol decreased CYP3A4 protein levels in a dose-dependent

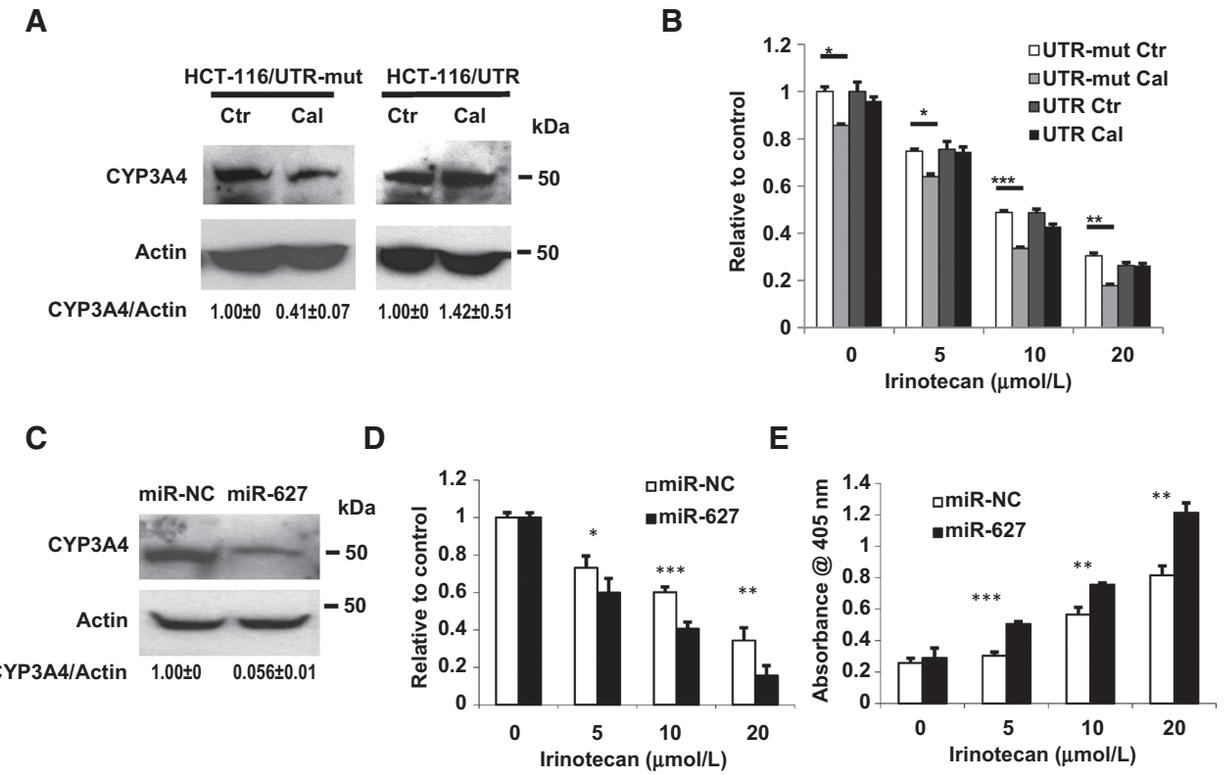

Figure 4.

miR-627 is required for the activity of calcitriol in enhancing the efficacy of irinotecan. **A,** HCT-116 cells stably transfected with pRNAT-CMV3.2/Puro-3′UTR (to overexpress 3′UTR sponge and block miR-627) or pRNAT-CMV3.2/Puro-3′UTR-mut (to overexpress 3′UTR sponge with miR-627 binding site mutation) were treated with 500 nmol/L calcitriol for 48 hours, and Western blots were done using the indicated antibodies. Relative protein levels were quantified and shown under the gel. The experiment was repeated 3 times. **B,** HCT-116 cells stably expressing the 3′UTR sponge (to block miR-627) or the 3′UTR sponge with miR-627 binding site mutation were treated with or without 500 nmol/L calcitriol for 24 hours, followed by treatment with various doses of irinotecan for 24 hours. The *in vitro* cell growth was analyzed using WST-1 assay. Value of the UTR-mut control (0.319) was set as 1. **C,** HCT-116 cells stably transfected with pcDNA6.2-GW/EmGFP-miR–negative control or pcDNA6.2-GW/EmGFP-miR-627 plasmids were analyzed by Western blots with the indicated antibodies. The experiment was repeated 3 times. **D** and **E,** HCT-116 cells stably expressing negative control miRNA or miR-627 were treated with various doses of irinotecan for 48 hours. **D,** cell proliferation was assessed by WST-1 assay as described in Materials and Methods. Value of the miR-NC control (0.458) was set as 1. **E,** apoptosis was assessed by Cell Death Detection Elisa assay as described in Materials and Methods. All of the above experiments have been repeated 3 times; data shown are mean values + SD (*, $P < 0.05$; **, $P < 0.01$; and ***, $P < 0.001$).

manner in HT-29 cells (Fig. 1D). Similarly, calcitriol was able to reduce CYP3A4 levels in HCT-116 cells (Supplementary Fig. S1).

Calcitriol and miR-627 inhibit intratumoral CYP3A4-mediated irinotecan metabolism and enhance the *in vitro* antitumor activity of irinotecan

Irinotecan is metabolized by CYP3A4 into the inactive metabolites NPC and APC (12). Since calcitriol decreases CYP3A4 protein, we examined the effects of calcitriol on irinotecan metabolism within the colon cancer cells. As shown in Fig. 2A, calcitriol inhibited CYP3A4-mediated metabolism of irinotecan in HT-29 cells. The levels of metabolic products of irinotecan (NPA and APC) were decreased after calcitriol treatment, and the levels of irinotecan were increased. Calcitriol also inhibited irinotecan metabolism by CYP3A4 in HCT-116 cells (Fig. 2B). While it has been shown that irinotecan induces CYP3A4 expression through steroid and xenobiotic receptor signaling (13), we found that CYP3A4 was suppressed by calcitriol and irinotecan combination treatment (Supplementary Fig. S2). Similarly, overexpression of exogenous miR-627 also decreased the levels of NPC and APC (Fig. 2C), whereas the levels of irinotecan were increased. We hypothesized that by inhibiting CYP3A4-mediated inactivation of irinotecan, calcitriol should increase the therapeutic efficacy of irinotecan. To test this, we treated HT-29 cells first with calcitriol for 24 hours, followed by treatment with various doses of irinotecan. As shown in Fig. 3A, pretreatment with calcitriol enhanced the activity of irinotecan in suppression of colon cancer cell proliferation. In addition, pretreatment of calcitriol also increased irinotecan-induced apoptosis (Fig. 3B). We also observed similar results in HCT-116 cell. Pretreatment with calcitriol increased the activity of irinotecan in growth suppression and induction of apoptosis (Fig. 3C and D). Using the CalcuSyn software, we found that the combination of calcitriol and irinotecan was synergistic (CI < 1) at all doses in HCT-116 and HT-29 cells (Supplementary Fig. S3).

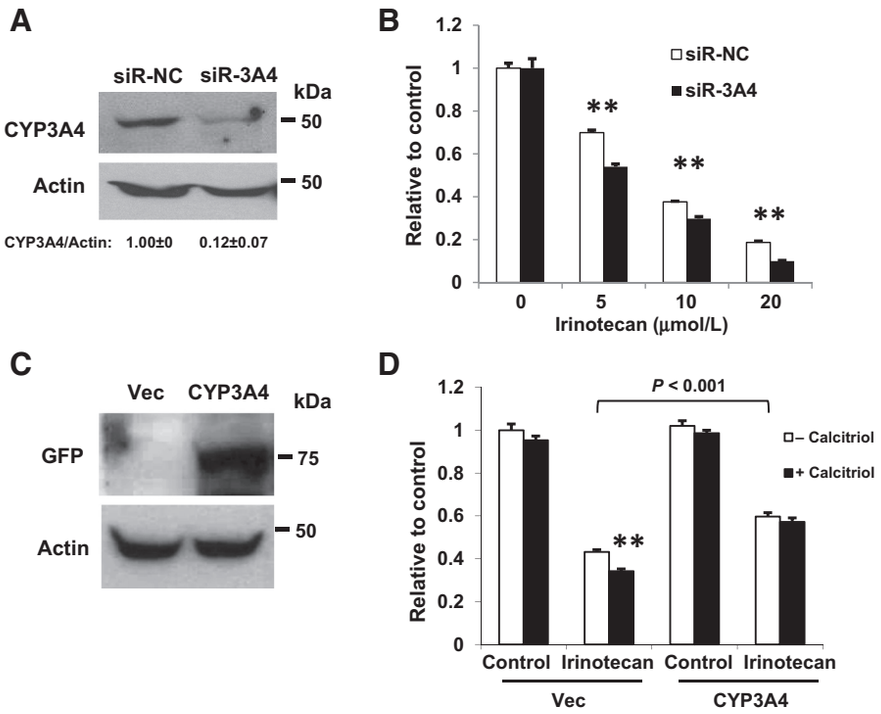

Figure 5.
CYP3A4 reduces the efficacy of irinotecan in colon cancer cells. **A,** HT-29 cells were transfected with the negative control or CYP3A4-targeting siRNAs. Knockdown of CYP3A4 protein was confirmed by Western blot. **B,** HT-29 cells were transfected with the negative control or CYP3A4-targeting siRNAs. At 24 hours after siRNA transfection, cells were treated with various doses of irinotecan for additional 24 hours. Cell proliferation was measured by WST-1 assay. Value of the siR-NC control (0.353) was set as 1. **C,** HCT-116 cells were transfected with the empty expression vector or pEGFP-CYP3A4. Overexpression of CYP3A4 was confirmed by Western blot. **D,** HCT-116 cells were transfected with the empty expression vector or pEGFP-CYP3A4. At 24 hours after transfection, cells were treated with or without 200 nmol/L of calcitriol for 24 hours, followed by 10 μmol/L of irinotecan for additional 24 hours. Cell proliferation was measured by WST-1 assay. Value of the control (0.507) was set as 1. The experiments have been repeated 3 times; data shown are mean values + SD. **, $P < 0.01$.

miR-627 is necessary and sufficient to enhance the antitumor activity of irinotecan

To further determine the role of miR-627 in calcitriol's enhancement of irinotecan's antitumor activity, we overexpressed a cDNA fragment containing a miR-627 target sequence (part of the 3′UTR of *JMJD1A* gene; ref. 18) in HCT-116 cells. The overexpressed mRNA containing the miR-627 target sequence (driven by a strong CMV promoter) would serve as a "sponge" to sequester and block the activity of miR-627. We employed this miRNA sponge strategy (33, 34) to create HCT-116 cell lines stably expressing the 3′UTR-derived miR-627 sponge for *in vitro* and *in vivo* studies. When miR-627 was blocked by the sponge, calcitriol failed to suppress the expression of CYP3A4 (Fig. 4A). As a result, calcitriol was no longer able to enhance the activity of irinotecan in suppression of cancer cell proliferation (Fig. 4B), indicating that induction of miR-627 is critical to the action of calcitriol in promoting irinotecan's activity. In contrast, when the miR-627 binding site was mutated and the sponge did not block miR-627, calcitriol was still able to decrease CYP3A4 (Fig. 4A) and enhance the antitumor activity of irinotecan (Fig. 4B). To determine if miR-627 alone is sufficient to increase the antitumor activity of irinotecan, we created HCT-116 cells stably expressing miR-627. As shown in Fig. 4C, stable expression of miR-627 was able to decrease the expression of CYP3A4. Furthermore, miR-627 expression increased the effects of irinotecan in suppressing cancer cell proliferation (Fig. 4D) and induction of apoptosis (Fig. 4E). Although miR-627 decreased the expression of CYP3A4 to a greater degree than calcitriol did, we did not observe a more pronounced effect on enhancing irinotecan in growth suppression or induction of apoptosis (when compared with the effects of calcitriol). Overexpression of miR-627 may target other mRNAs that can potentially interfere with the effect on irinotecan.

CYP3A4 is a critical target in calcitriol's enhancement of the antitumor activity of irinotecan

To further determine the role of CYP3A4 in the antitumor activity of irinotecan, we specifically knocked down CYP3A4 using siRNA. As shown in Fig. 5A and B, siRNA knockdown of CYP3A4 significantly increased the efficacy of irinotecan in suppressing the proliferation of HT-29 cells (which express relatively higher level of CYP3A4 than HCT-116 cells, data not shown). The effects of CYP3A4 siRNA knockdown on irinotecan were validated using another siRNA targeting different site of the CYP3A4 mRNA (Supplementary Fig. S4). We have previously shown that miR-627–mediated downregulation of JMJD1A is involved in the antitumor activity of calcitriol (18). To eliminate the possibility that calcitriol may enhance the activity of irinotecan through JMJD1A, we isolated CD133-negative cells from HCT-116. It was shown previously that only the CD133-positive HCT-116 cells express JMJD1A, and $CD133^-$ HCT-116 cells express minimal level of JMJD1A (35). We found that about 29.7% of the HCT-116 population are CD133 positive and confirmed that $CD133^-$ HCT-116 cells express very low level of JMJD1A (see below). In the isolated $CD133^-$ HCT-116 cells, when we knocked down CYP3A4 with siRNA, calcitriol was no longer able to enhance the activity of irinotecan (Supplementary Fig. S5). On the other hand, when we overexpressed CYP3A4 in the HCT-116 cells, we found that the effect of calcitriol on enhancing irinotecan-mediated growth suppression was abolished (Fig. 5C and D). VDR expression and signaling were retained in CYP3A4-overexpressing HCT-116 cells (Supplementary Fig. S6). Silencing of CYP3A4 in HCT-116 cells reduced irinotecan metabolism and increased irinotecan level, whereas CYP3A4 overexpression increased irinotecan metabolism and decreased irinotecan level (Supplementary Fig. S7).

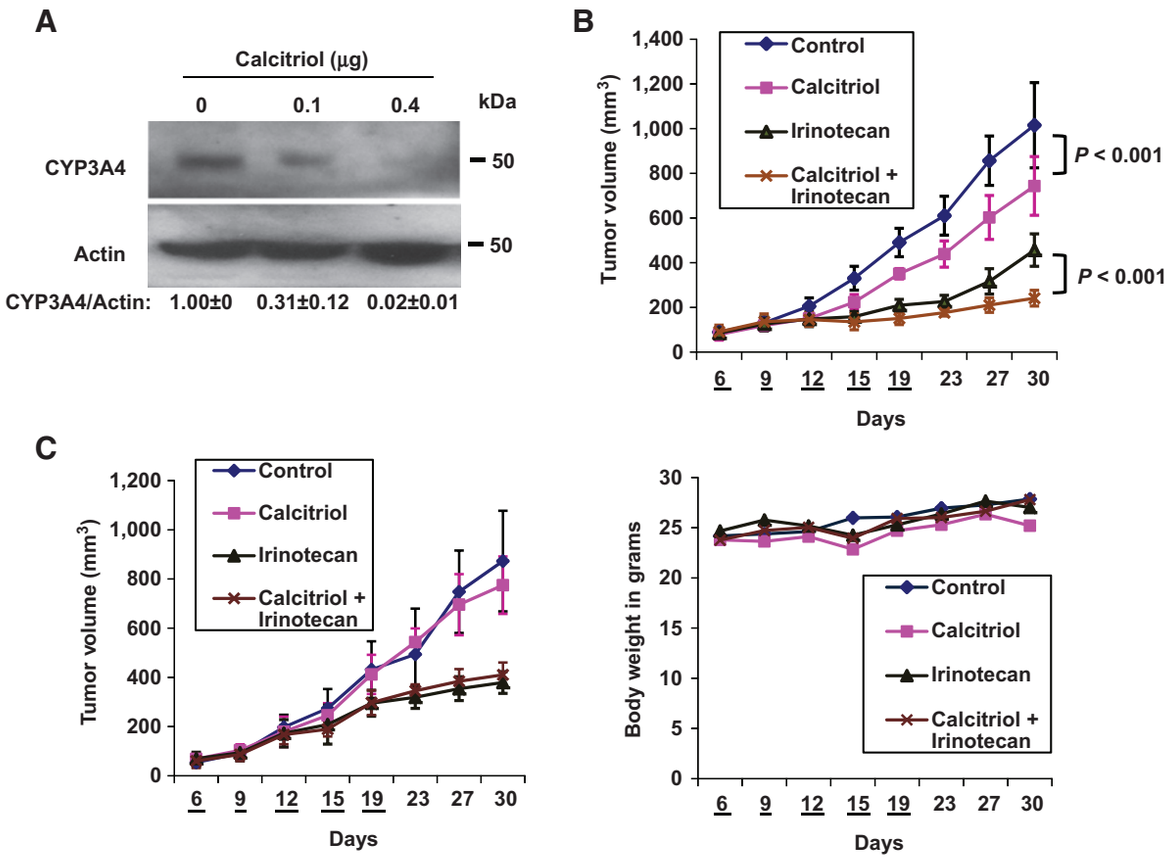

Figure 6.

Calcitriol downregulates CYP3A4 and enhances the *in vivo* antitumor activity of irinotecan. **A,** nude mice bearing HT-29 tumor xenografts were treated with calcitriol at i.p. doses of 0.1 and 0.4 μg daily for 2 days. Tumor samples were collected 24 hours after the second dose and analyzed by Western blotting with the indicated antibodies. The experiments have been repeated 3 times. **B,** nude mice bearing HCT-116-3′UTR-mut xenografts (expressing the 3′UTR sponge with the miR-627 binding site mutated, as control) were treated with calcitriol (0.4 μg), irinotecan (50 mg/kg), calcitriol (0.4 μg) plus irinotecan (50 mg/kg), or DMSO for the control group ($n = 8$ per group). Treatments were given on the underlined days. Tumor volumes and body weights were measured at indicated time points. **C,** nude mice bearing HCT-116-3′UTR xenografts (transfected with pRNAT-CMV3.2/Puro-3′UTR to stably express the 3′UTR sponge to block miR-627) were treated with calcitriol, irinotecan, calcitriol plus irinotecan (the same doses and schedule as described in **B**), or DMSO ($n = 8$ per group). Tumor volumes were measured.

Calcitriol enhances the *in vivo* antitumor activity of irinotecan through induction of miR-627

We have previously demonstrated that calcitriol induces miR-627 expression *in vivo* in a nude mouse xenograft model (18). To determine if calcitriol decreases CYP3A4 (through miR-627) expression *in vivo*, we established human colon cancer xenografts in nude mice and treated the mice with calcitriol. As shown in Fig. 6A, calcitriol decreased CYP3A4 expression *in vivo* in the tumor xenografts. In mice bearing xenografts of HCT-116 cells expressing the mutated 3′UTR sponge (as control), at the dose of 0.4 μg (which does not induce hypercalcemia in mice; ref. 36), calcitriol enhanced the antitumor activity of irinotecan in suppressing tumor growth in the nude mice, without inducing any toxicity (measured by the loss of body weight), as shown in Fig. 6B. We did not observe any symptoms of toxicity in the mice (lethargy, decreased feeding, etc.). In contrast, when we blocked the activity of miR-627 using the 3′UTR sponge which can sequester miR-627 and calcitriol was no longer able to decrease CYP3A4 (Fig. 4A), not only did calcitriol fail to suppress xenograft growth, but also it failed to enhance the activity of irinotecan in tumor suppression in the nude mice (Fig. 6C). After isolation of CD133$^-$ HCT-116 cells (29.7% of the HCT-116 population are CD133 positive, Fig. 7A) that express minimal level of JMJD1A (Fig. 7B; ref. 35), we established CD133$^-$ HCT-116 xenografts in nude mice. As shown in Fig. 7, calcitriol decreased CYP3A4 (Fig. 7B, bottom) and enhanced the activity of irinotecan in tumor suppression in the CD133$^-$ HCT-116 xenografts. Thus, induction of miR-627 and the subsequent reduction of CYP3A4 are critical for the activity of calcitriol in promoting the efficacy of irinotecan. In addition, we found that while a lower dose of calcitriol did not have antitumor activity itself, it was sufficient to enhance the antitumor activity of a low-dose irinotecan treatment (Supplementary Fig. S8). Calcitriol treatment increased the intratumoral level of irinotecan (Supplementary Fig. S9A). At 0.4 μg, calcitriol did not increase the blood calcium level above the reference range (8.0–15.5 mg/dL; ref. 37), as shown in Supplementary Fig. S9B.

Discussion

Drug resistance is a major problem in cancer chemotherapy (38). Multiple mechanisms have been intensively studied to

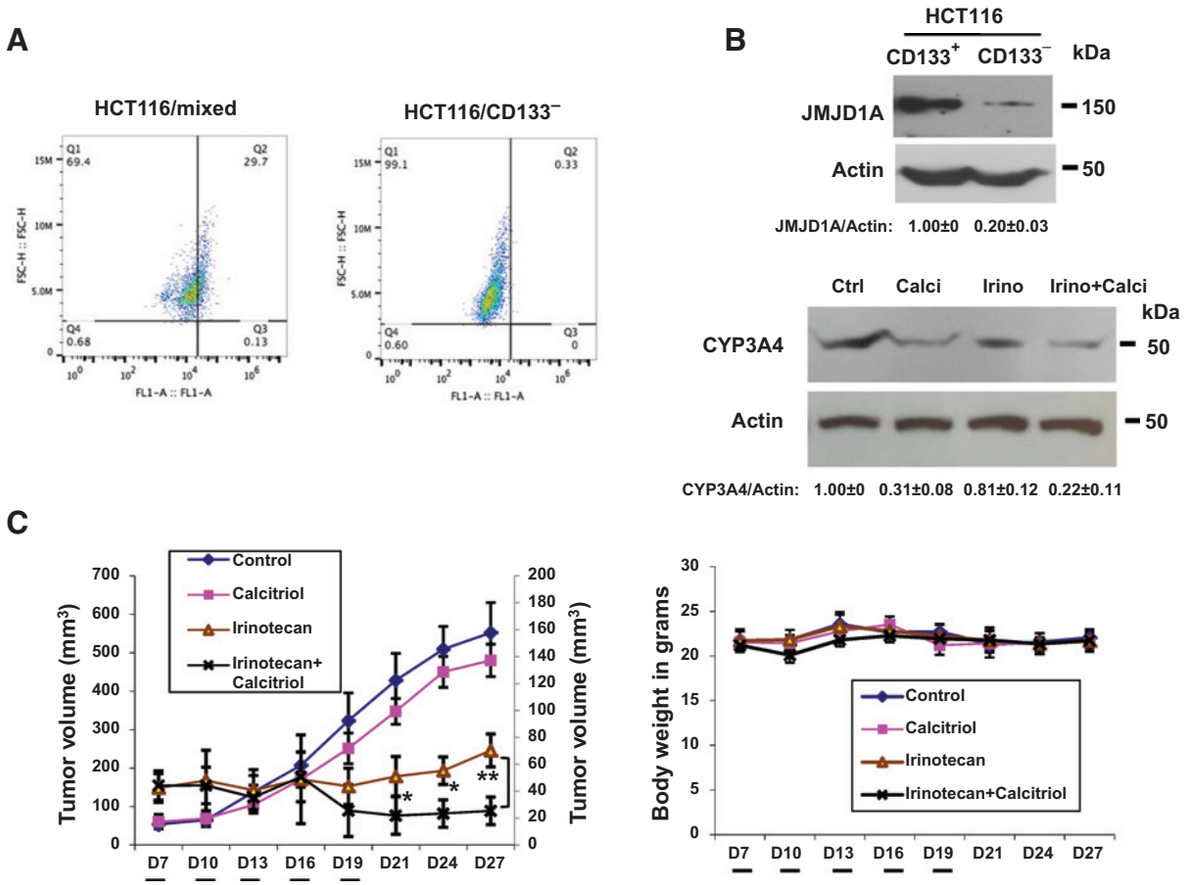

Figure 7.

Calcitriol enhances the antitumor activity of irinotecan in CD133⁻ HCT-116 xenografts. **A,** the CD133⁻ cells were isolated by removing CD133-positive cells using the EasySep Selection Kit. The purity of cell isolation was verified by flow cytometry. **B,** after CD133⁻ cells were separated from the CD133-positive cells, cell lysates were analyzed by Western blots with the indicated antibodies (top). Bottom, nude mice bearing CD133⁻ HCT-116 xenografts were treated as in **C**. Tumor samples were collected at the end of experiments and analyzed by Western blotting with the indicated antibodies. The experiment was repeated 3 times. **C,** nude mice bearing CD133⁻ HCT-116 xenografts were treated with calcitriol (0.4 μg), irinotecan (50 mg/kg), calcitriol (0.4 μg) plus irinotecan (50 mg/kg), or DMSO for the control group ($n = 8$ per group). Treatments were given on the underlined days. Tumor volumes and body weights were measured at the indicated time points. The data of the irinotecan and calcitriol/irinotecan combination groups were plotted with a different scale using the right axis, (*, $P < 0.05$ and **, $P < 0.01$).

understand the causes of drug resistance. Although most of previous studies have focused on multidrug resistance genes (such as P-glycoprotein; ref. 39), antiapoptotic genes (40), and overexpression/amplification of drug targets (41, 42), few attention was given to drug metabolism as a mechanism for drug resistance. Studies to identify a solution to metabolism-mediated drug resistance were even rare. In this study, we have demonstrated that CYP3A4-mediated metabolism of irinotecan can potentially serve as a mechanism of drug resistance. More importantly, miR-627–mediated downregulation of CYP3A4 can provide a mechanism to overcome such resistance to irinotecan. By activating miR-627, calcitriol can be employed to enhance the anticancer activity of irinotecan, a major therapeutic agent for colon cancer. Thus, our findings provide an effective solution to the intratumoral inactivation of irinotecan by CYP3A4, i.e., using the widely available vitamin D to downregulate CYP3A4 and improve the efficacy of irinotecan.

CYP3A4 is a major drug metabolism enzyme expressed in the liver (43). Interestingly, previous studies have demonstrated that vitamin D induces CYP3A4 expression in the liver (44). This opposite effect of vitamin D on CYP3A4 in the liver can be utilized to the benefit of reducing the systemic toxicities of irinotecan. In fact, irinotecan has three main dose-limiting toxicities: myelosuppression, diarrhea, and neutropenia. About 70% of patients receiving irinotecan treatment suffer from diarrhea, which makes an increased dosing schedule difficult (45). Approximately 55% of these patients have to receive a lower dose than scheduled after 1 month. While vitamin D induces CYP3A4 in the liver to reduce systemic exposure of irinotecan (thus reducing toxicity), it decreases CYP3A4 in the colon cancer cells (thus increasing the efficacy of irinotecan). As a result, it may even be possible to increase the dose of irinotecan higher than the normal MTD, because vitamin D has selectively decreased systemic exposure while increasing the intratumoral drug concentration.

It has been shown previously that CYP3A4 expression in the established colon cancer cell lines (including HT-29 and HCT-116) is relatively low due to promoter methylation-mediated epigenetic silencing (46). In contrast, CYP3A4 expression and

enzyme activity in the primary human colon cancer samples are high (at similar or higher levels than that in the liver; refs. 15, 47). Thus, CYP3A4 may have an even more profound effect on irinotecan's antitumor activity in the primary colon cancer samples. In future studies using the mouse tumorgraft model that carries primary patient-derived colon cancers, we anticipate to observe more significant enhancement of irinotecan's activity when vitamin D is used to downregulate CYP3A4.

Our data indicate that induction of miR-627 expression may serve as an important mechanism of vitamin D in modulating the intratumoral CYP3A4 activity in colon cancer. Strategies to selectively deliver miR-627- or CYP3A4-targeting siRNA may prove to be effective to reduce the CYP3A4 level in cancer cells and improve tumor response to irinotecan.

Disclosure of Potential Conflicts of Interest

No potential conflicts of interest were disclosed.

Authors' Contributions

Conception and design: M. Sun, B. Guo
Development of methodology: M. Sun, X. Yang, S.Y. Qian, B. Guo
Acquisition of data (provided animals, acquired and managed patients, provided facilities, etc.): M. Sun, Q. Zhang, X. Yang, S.Y. Qian
Analysis and interpretation of data (e.g., statistical analysis, biostatistics, computational analysis): M. Sun, S.Y. Qian, B. Guo
Writing, review, and/or revision of the manuscript: Q. Zhang, B. Guo
Administrative, technical, or material support (i.e., reporting or organizing data, constructing databases): M. Sun, Q. Zhang, B. Guo
Study supervision: S.Y. Qian, B. Guo

Grant Support

This work was supported by the NIH (CA186100 and GM114080 to B. Guo).

The costs of publication of this article were defrayed in part by the payment of page charges. This article must therefore be hereby marked *advertisement* in accordance with 18 U.S.C. Section 1734 solely to indicate this fact.

Received February 19, 2016; revised June 30, 2016; accepted July 4, 2016; published OnlineFirst July 25, 2016.

References

1. Cole SP. Targeting multidrug resistance protein 1 (MRP1, ABCC1): Past, present, and future. Annu Rev of Pharmacol and Toxicol 2014;54:95–117.
2. Sharom FJ. The P-glycoprotein multidrug transporter. Essays Biochem 2011;50:161–78.
3. Reed JC. Bcl-2 family proteins: Regulators of chemoresistance in cancer. Toxicol Lett 1995;82-83:155–8.
4. Banerjee D, Ercikan-Abali E, Waltham M, Schnieders B, Hochhauser D, Li WW, et al. Molecular mechanisms of resistance to antifolates, a review. Acta Biochim Pol 1995;42:457–64.
5. Guengerich FP. Cytochrome P-450 3A4: Regulation and role in drug metabolism. Annu Rev Pharmacol Toxicol 1999;39:1–17.
6. Rodriguez-Antona C, Leskela S, Zajac M, Cuadros M, Alves J, Moneo MV, et al. Expression of CYP3A4 as a predictor of response to chemotherapy in peripheral T-cell lymphomas. Blood 2007;110:3345–51.
7. Xu J, Wang J, Hu Y, Qian J, Xu B, Chen H, et al. Unequal prognostic potentials of p53 gain-of-function mutations in human cancers associate with drug-metabolizing activity. Cell Death Dis 2014;5:e1108.
8. Assis J, Pereira D, Gomes M, Marques D, Marques I, Nogueira A, et al. Influence of CYP3A4 genotypes in the outcome of serous ovarian cancer patients treated with first-line chemotherapy: Implication of a CYP3A4 activity profile. Int J Clin Exp Med 2013;6:552–61.
9. Sakurai K, Enomoto K, Matsuo S, Amano S, Shiono M. CYP3A4 expression to predict treatment response to docetaxel for metastasis and recurrence of primary breast cancer. Surg Today 2011;41:674–9.
10. Yao D, Ding S, Burchell B, Wolf CR, Friedberg T. Detoxication of vinca alkaloids by human P450 CYP3A4-mediated metabolism: implications for the development of drug resistance. J Pharmacol Exp Ther 2000;294: 387–95.
11. Aggarwal S, Chu E. Current therapies for advanced colorectal cancer. Oncology (Williston Park) 2005;19:589–95.
12. Mathijssen RH, van Alphen RJ, Verweij J, Loos WJ, Nooter K, Stoter G, et al. Clinical pharmacokinetics and metabolism of irinotecan (CPT-11). Clin Cancer Res 2001;7:2182–94.
13. Basseville A, Preisser L, de Carne Trecesson S, Boisdron-Celle M, Gamelin E, Coqueret O, et al. Irinotecan induces steroid and xenobiotic receptor (SXR) signaling to detoxification pathway in colon cancer cells. Mol Cancer 2011;10:80.
14. Olszewski U, Liedauer R, Ausch C, Thalhammer T, Hamilton G. Overexpression of CYP3A4 in a COLO 205 colon cancer stem cell model in vitro. Cancers 2011;3:1467–79.
15. Canaparo R, Nordmark A, Finnstrom N, Lundgren S, Seidegard J, Jeppsson B, et al. Expression of cytochromes P450 3A and P-glycoprotein in human large intestine in paired tumour and normal samples. Basic Clin Pharmacol Toxicol 2007;100:240–8.
16. Deeb KK, Trump DL, Johnson CS. Vitamin D signalling pathways in cancer: Potential for anticancer therapeutics. Nat Rev Cancer 2007;7:684–700.
17. Milczarek M, Rosinska S, Psurski M, Maciejewska M, Kutner A, Wietrzyk J. Combined colonic cancer treatment with vitamin D analogs and irinotecan or oxaliplatin. Anticancer Res 2013;33:433–44.
18. Padi SK, Zhang Q, Rustum YM, Morrison C, Guo B. MicroRNA-627 mediates the epigenetic mechanisms of vitamin D to suppress proliferation of human colorectal cancer cells and growth of xenograft tumors in mice. Gastroenterology 2013;145:437–46.
19. Bartel DP. MicroRNAs: Target recognition and regulatory functions. Cell 2009;136:215–33.
20. Carleton M, Cleary MA, Linsley PS. MicroRNAs and cell cycle regulation. Cell Cycle 2007;6:2127–32.
21. Kota J, Chivukula RR, O'Donnell KA, Wentzel EA, Montgomery CL, Hwang HW, et al. Therapeutic microRNA delivery suppresses tumorigenesis in a murine liver cancer model. Cell 2009;137:1005–17.
22. Chen CZ, Li L, Lodish HF, Bartel DP. MicroRNAs modulate hematopoietic lineage differentiation. Science 2004;303:83–6.
23. Zhang J, Jima DD, Jacobs C, Fischer R, Gottwein E, Huang G, et al. Patterns of microRNA expression characterize stages of human B-cell differentiation. Blood 2009;113:4586–94.
24. Poy MN, Eliasson L, Krutzfeldt J, Kuwajima S, Ma X, Macdonald PE, et al. A pancreatic islet-specific microRNA regulates insulin secretion. Nature 2004;432:226–30.
25. Hartig SM, Hamilton MP, Bader DA, McGuire SE. The miRNA Interactome in metabolic homeostasis. Trends Endocrinol Metab: TEM 2015;26:733–45.
26. Valastyan S, Weinberg RA. miR-31: A crucial overseer of tumor metastasis and other emerging roles. Cell Cycle 2010;9:2124–9.
27. Ma L, Teruya-Feldstein J, Weinberg RA. Tumour invasion and metastasis initiated by microRNA-10b in breast cancer. Nature 2007;449:682–8.
28. Hermeking H. The miR-34 family in cancer and apoptosis. Cell Death Differ 2010;17:193–9.
29. Bhatnagar N, Li X, Padi S, Zhang Q, Tang M, Guo B. Downregulation of miR-205 and miR-31 confers resistance to chemotherapy-induced apoptosis in prostate cancer cells. Cell Death Dis 2010;1;e105.
30. Xu Y, Qi J, Yang X, Wu E, Qian SY. Free radical derivatives formed from cyclooxygenase-catalyzed dihomo-gamma-linolenic acid peroxidation can attenuate colon cancer cell growth and enhance 5-fluorouracil's cytotoxicity. Redox Biol 2014;2:610–8.
31. Marangon E, Posocco B, Mazzega E, Toffoli G. Development and validation of a high-performance liquid chromatography-tandem mass spectrometry method for the simultaneous determination of irinotecan and its main metabolites in human plasma and its application in a clinical pharmacokinetic study. PloS ONE 2015;10:e0118194.
32. Wei Z, Jiang S, Zhang Y, Wang X, Peng X, Meng C, et al. The effect of microRNAs in the regulation of human CYP3A4: A systematic study using a mathematical model. Sci Rep 2014;4:4283.

33. Ebert MS, Sharp PA. MicroRNA sponges: Progress and possibilities. RNA 2010;16:2043–50.
34. Kluiver J, Slezak-Prochazka I, Smigielska-Czepiel K, Halsema N, Kroesen BJ, van den Berg A. Generation of miRNA sponge constructs. Methods 2012;58:113–7.
35. Yang J, Ledaki I, Turley H, Gatter KC, Montero JC, Li JL, et al. Role of hypoxia-inducible factors in epigenetic regulation via histone demethylases. Ann N Y Acad Sci 2009;1177:185–97.
36. Muindi JR, Modzelewski RA, Peng Y, Trump DL, Johnson CS. Pharmacokinetics of 1alpha,25-dihydroxyvitamin D3 in normal mice after systemic exposure to effective and safe antitumor doses. Oncology 2004;66:62–6.
37. http://cal.vet.upenn.edu/ [Internet]. Pennsylvania: University of Pennsylvania School of Veterinary Medicine; c2002 [updated 2003 May 31; cited 2016 Jun 28]. Available from: http://cal.vet.upenn.edu/projects/ssclinic/refdesk/rodentrr.htm.
38. Holohan C, Van Schaeybroeck S, Longley DB, Johnston PG. Cancer drug resistance: An evolving paradigm. Nat Rev Cancer 2013;13:714–26.
39. Ling V. Multidrug resistance: molecular mechanisms and clinical relevance. Cancer Chemother Pharmacol 1997;40 Suppl:S3–8.
40. Reed JC. Dysregulation of apoptosis in cancer. J Clin Oncol 1999;17:2941–53.
41. Hopper-Borge EA, Nasto RE, Ratushny V, Weiner LM, Golemis EA, Astsaturov I. Mechanisms of tumor resistance to EGFR-targeted therapies. Expert Opin Ther Targets 2009;13:339–62.
42. Hait WN. Anticancer drug development: The grand challenges. Nat Rev Drug Discov 2010;9:253–4.
43. Li AP, Kaminski DL, Rasmussen A. Substrates of human hepatic cytochrome P450 3A4. Toxicology 1995;104:1–8.
44. Khan AA, Chow EC, van Loenen-Weemaes AM, Porte RJ, Pang KS, Groothuis GM. Comparison of effects of VDR versus PXR, FXR and GR ligands on the regulation of CYP3A isozymes in rat and human intestine and liver. Eur J Pharm Sci 2009;37:115–25.
45. Marcuello E, Altes A, Menoyo A, Del Rio E, Gomez-Pardo M, Baiget M. UGT1A1 gene variations and irinotecan treatment in patients with metastatic colorectal cancer. Br J Cancer 2004;91:678–82.
46. Habano W, Gamo T, Terashima J, Sugai T, Otsuka K, Wakabayashi G, et al. Involvement of promoter methylation in the regulation of Pregnane X receptor in colon cancer cells. BMC Cancer 2011;11:81.
47. Martinez C, Garcia-Martin E, Pizarro RM, Garcia-Gamito FJ, Agundez JA. Expression of paclitaxel-inactivating CYP3A activity in human colorectal cancer: Implications for drug therapy. Br J Cancer 2002;87:681–6.